

# Electrocatalytic oxidation of methanol on carbon ceramic electrode modified by platinum nanoparticles incorporated in poly (*o*-phenylenediamine) film

H. Razmi · E. Habibi

Received: 21 August 2008 / Revised: 30 October 2008 / Accepted: 13 November 2008 / Published online: 13 December 2008  
© Springer-Verlag 2008

**Abstract** Carbon ceramic electrode, a new electrode substrate, was prepared by sol–gel procedure and used for the electropolymerization of *o*-phenylenediamine and incorporation of platinum nanoparticles into the resulting poly(*o*-phenylenediamine) (PoPD) film. The modified electrode was used for electrooxidation of methanol in 0.3 M H<sub>2</sub>SO<sub>4</sub> as supporting electrolyte. The presence of PoPD film increased considerably the efficiency of deposited Pt nanoparticles toward the electrocatalytic oxidation of methanol. The effective parameters on the electrooxidation of methanol, i.e., amounts of polymer and Pt catalyst, medium temperature, working potential limit in anodic direction, and potential scan rate, were investigated, and the results were discussed.

**Keywords** Carbon ceramic electrode · Methanol oxidation · Platinum nanoparticles · Poly(*o*-phenylenediamine)

## Introduction

Recently, direct alcohol fuel cells (DAFCs), due to their relatively high specific energy, easy handling, low price, and easy accessibility are considered as among the power sources for both stationary and portable devices [1]. Among several alcohols which can be used in a DAFC, methanol is generally considered as the most appropriate fuel because it is a liquid fuel of relatively high activity in fuel cell systems [1] and can be nearly completely electro-

oxidized to the final product of CO<sub>2</sub> due to its simple molecular structure [2].

Platinum or platinum-based materials are the best anodic materials that exhibit catalytic properties for the oxidation process of alcohols to proceed at a sufficient rate in fuel cells [3–6], but the very high cost of these electrocatalysts is not economic in the fabrication of components for these fuel cells. Apart from high cost, Pt can be easily poisoned by the strongly adsorbed CO species that are formed from incomplete oxidation of alcohols in anodic reaction [7, 8]. Incorporation of Pt particles into conducting polymer-coated electrode increases the electrocatalytic activity of Pt particles for the electrooxidation of organic fuels by decreasing the poisoning phenomena [9–11], which is caused by high dispersion of Pt particles in polymer matrix and the synergistic effects of conducting polymer and metal particles [12, 13]. The used polymers are polyaniline [14–17], polypyrrole [18, 19], and polythiophene [20–22]. These polymers offer great advantages due to their very good conducting and mechanical properties. However, there is increasing interest to extend such studies to other polymers, which might be suitable as host material of the catalyst particles. One of these kinds of polymers is poly(*o*-phenylenediamine) (PoPD). Electrooxidation of methanol on different substrates modified with platinum particles dispersed on PoPD film were extensively studied [10, 23, 24].

In this work, considering stability, high conductivity, simplicity, low cost, easy production, and porosity of carbon ceramic electrode (CCE) [25–29], we used it as substrate for electrochemical preparation of PoPD film. After preparation of PoPD|CCE, Pt nanoparticles were incorporated into the polymer film, and a Pt|PoPD|CCE was obtained. The Pt|PoPD|CCE was used for the electrooxidation of methanol in aqueous acidic solutions. For

H. Razmi (✉) · E. Habibi  
Electrochemistry Research Lab., Faculty of Sciences,  
Azarbaijan University of Tarbiat Moallem,  
P.O. Box: 53714-161, Tabriz, Iran  
e-mail: h.razmi@azaruniv.edu

comparison, the cyclic voltammogram of methanol oxidation on the Pt|CCE is also presented.

## Experimental

The electrochemical experiments were performed with an AUTOLAB PGSTAT-100 (potentiostat/galvanostat) equipped with a Universal Serial Bus (USB) electrochemical interface and driven GPES software. A conventional three-electrode cell was used at room temperature. A carbon ceramic electrode-modified platinum particle (Pt|CCE), poly(*o*-phenylenediamine), (PoPD|CCE), or platinum dispersed PoPD film (Pt|PoPD|CCE) was used as working electrode. A saturated calomel electrode (Hg|Hg<sub>2</sub>Cl<sub>2</sub>, 3 M KCl) and a platinum wire were used as the reference and auxiliary electrodes, respectively. JULABO thermostat was used to control cell temperature. The scanning electron microscopy (SEM) and energy dispersive X-ray (EDX) analyses were also carried out by using a scanning electron microscope LEO 440i Oxford equipped with EDX microanalyzer.

Pt and Pt|PoPD electrocatalysts were prepared on the CCE surface in solution of 0.3 M H<sub>2</sub>SO<sub>4</sub> (Merck) containing 0.002 M H<sub>2</sub>PtCl<sub>6</sub> (Merck) as Pt source. The preparation of CCE consists of the following steps: The amount of 0.9 mL methyltrimethoxysilane (Fluka) was mixed with 0.6 mL methanol (Merck). After addition of 0.6 mL 0.5 M HCl (Merck) as catalyst, the mixture was magnetically stirred (for about 15 min). Then, 0.3 g graphite powder (Merck) was added, and the mixture was firmly packed into a Teflon tube and dried for at least 24 h at room temperature.

After preparation of CCE, it was immersed in an aqueous solution of 0.3 M H<sub>2</sub>SO<sub>4</sub> containing 40 mM *o*-phenylenediamine (Merck), and its surface was coated with poly(*o*-phenylenediamine) film via an electropolymerization process which occurred by cycling the electrode potential between −0.4 and 1.3 V vs. SCE at scan rate of 50 mV s<sup>−1</sup>.

The amount of deposited polymer at the surface of CCE can be calculated from the charge consumed (*Q*) during the electrodeposition of PoPD film (the overall charge that passed during the anodic sweeps of potential) using Faraday's law. A value of 2 for *n*, 108 for *o*-phenylenediamine (*o*PD) molecular weight, 1.14 g cm<sup>−3</sup> for PoPD density and 0.119 cm<sup>2</sup> for the geometric surface area (*A<sub>g</sub>*) of the electrode were considered.

The platinum nanoparticles were potentiostatically deposited at the surface of CC and PoPD|CC electrodes (*A<sub>g</sub>*, 0.119 cm<sup>2</sup>) from an aqueous solution containing 0.002 M H<sub>2</sub>PtCl<sub>6</sub>+0.3 M H<sub>2</sub>SO<sub>4</sub> as supporting electrolyte. Electrodeposition of Pt was performed potentiostatically at −0.2 V vs. SCE. The amount of Pt deposited on the CCE and

PoPD|CCE was calculated from the charge consumed during the electrodeposition of Pt by using Faraday's law, considering a value of 4 for *n* according to the following faradic reaction:



## Results and discussion

*General aspects of electrooxidation of methanol* The electrooxidation of methanol was investigated at the carbon ceramic electrodes modified by Pt nanoparticles and a thin film of PoPD containing Pt nanoparticles. Our investigations showed that *o*PD can be electropolymerized at the surface of bare CCE. Figure 1 indicates the electropolymerization of *o*PD at the CCE by potentiodynamic method. As can be seen in Fig. 1, in the first anodic sweep, the oxidation of *o*PD occurs and an irreversible broad anodic peak appears at 1 V (peak a). In the first reverse cycle, some of the oxidation products of *o*PD is deposited on the electrode surface and the polymerization begins, and the new cathodic peak at −0.08 V appears (peak b), confirming the initial deposition of electro-oxidized products. In the second positive scan, there was an anodic peak at around −0.01 V (peak c). Along with the increase in the number of potential cycles, the anodic peak current for oxidation of *o*PD decreased significantly. This decrease in oxidation current is probably due to the loss of activity of the electrode surface when covered gradually with newly formed polymer film.

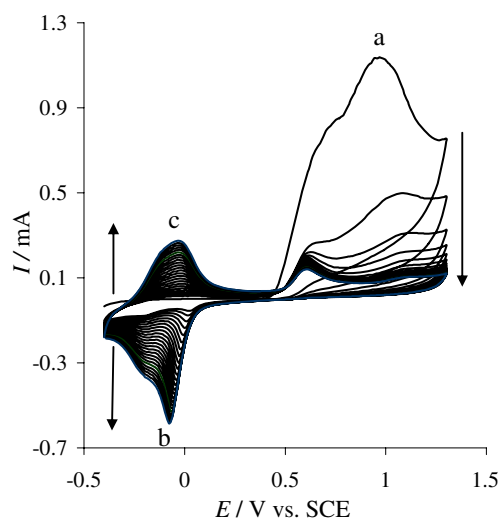


**Fig. 1** Cyclic voltammograms (25 cycles) recorded during potentiodynamic growth of PoPD film on CCE in solution containing 40 mM *o*-phenylenediamine and 0.3 M H<sub>2</sub>SO<sub>4</sub> at a scan rate of 50 mV s<sup>−1</sup>

Figure 2a shows the cyclic voltammogram of CCE modified with PoPD film with an optimum amount in 0.3 M H<sub>2</sub>SO<sub>4</sub> at scan rate of 50 mV s<sup>-1</sup>. According to Fig. 2a, the PoPD film showed redox activity in the range -0.4 to 0.15 V, and a wide electrochemical window from 0.15 to 1.3 V is available for electrocatalytic applications. By cycling the PoPD film repeatedly for about 200 times at scan rate of 50 mV s<sup>-1</sup>, the peak current value reduces less than 8%; this indicates a good stability.

A typical cyclic voltammogram of Pt|PoPD|CCE was shown in Fig. 2b. Peaks appeared at -279 mV (*c*<sub>1</sub>) and -100 mV (*c*<sub>2</sub>) in the cathodic and at -159 mV (*a*<sub>1</sub>) and -2 mV (*a*<sub>2</sub>) in the anodic directions are associated with the adsorption and desorption of hydrogen atoms on the platinum surface [30, 31]. The broad anodic peak at 760 mV (*a*<sub>3</sub>) and cathodic peak at 354 mV (*c*<sub>3</sub>) are related to the formation and reduction of platinum oxides, respectively [32].

The surface morphology of PoPD|CCE and Pt|PoPD|CCE has been investigated by SEM, and the corresponding micrographs were shown in Fig. 3a,b, respectively. As can be seen in Fig. 3a, the PoPD film with a uniform coverage and lumpy morphology are formed on the surface of carbon ceramic. The surface of PoPD|CCE is dense and scaly.

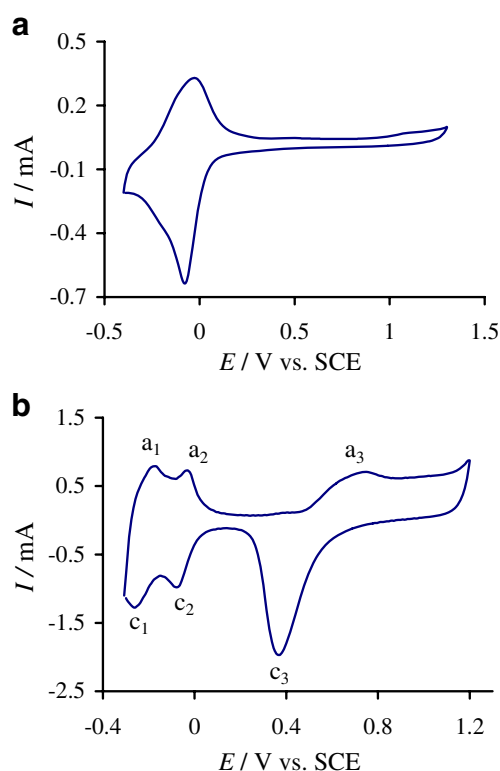


**Fig. 2** Cyclic voltammograms of **a** PoPD|CCE and **b** Pt|PoPD|CCE obtained in 0.1 M H<sub>2</sub>SO<sub>4</sub> electrolyte solution; the amount of deposited polymer, 66 μg cm<sup>-2</sup> and amount of Pt, 0.6 mg cm<sup>-2</sup>

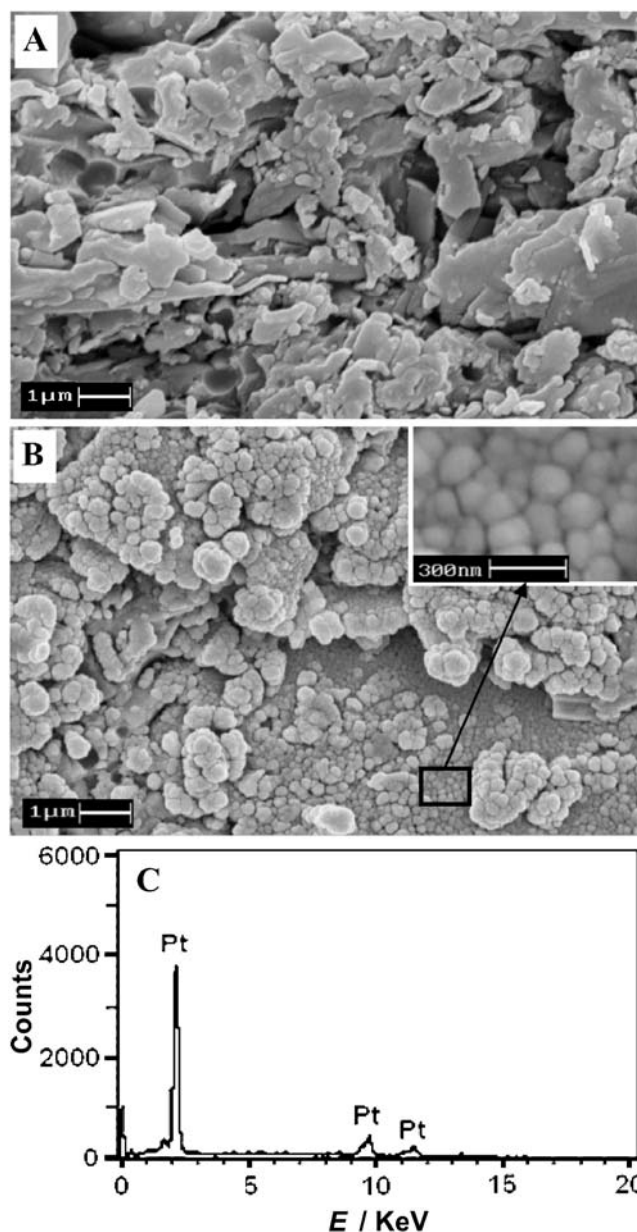


**Fig. 3** SEM images of **a** PoPD|CCE and **b** Pt|PoPD|CCE surfaces. **c** EDX spectra of Pt|PoPD|CCE. Amount of polymer and Pt were as in Fig. 2

After deposition of Pt on the polymer film, Pt particles are being formed in the shape of clews consisting of platinum crystallite aggregates (Fig. 3b). The size of these clews is in the range 100–150 nm. The obtained nanoparticles are well dispersed on the PoPD film. EDX results (Fig. 3c) confirmed that the distributions of platinum nanoparticles were achieved predominantly on the surface of PoPD.

Electrooxidation of methanol at platinum-based electrodes has been studied extensively [23, 32, 33]. Results from infra-red spectroscopy show that the methanol oxidation on

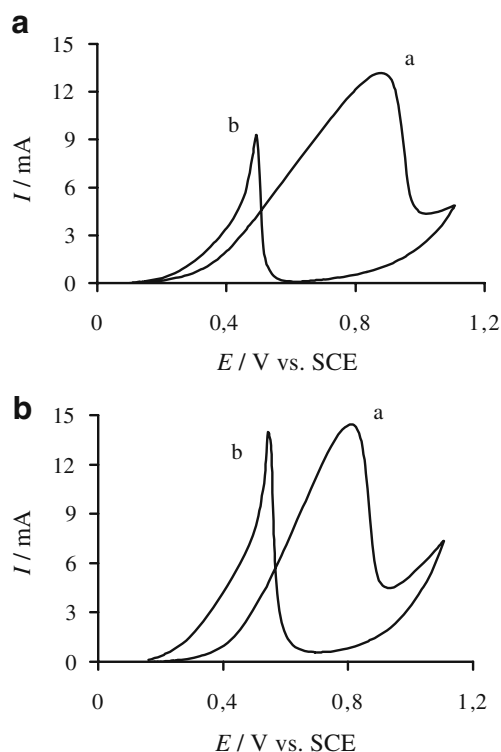
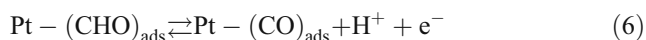
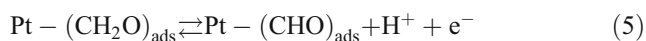
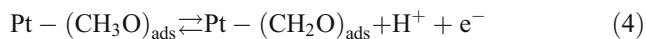
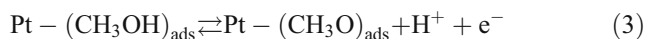
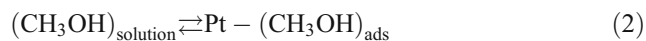


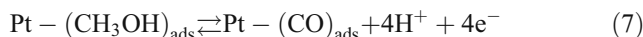
**Fig. 4** Cyclic voltammograms of 0.5 M methanol on **a** Pt|CCE with  $2 \text{ mg cm}^{-2}$  Pt and **b** Pt|PoPD|CCE in 0.3 M  $\text{H}_2\text{SO}_4$  at  $25^\circ\text{C}$  with scan rate of  $50 \text{ mV s}^{-1}$ ; the amount of deposited polymer,  $66 \mu\text{g cm}^{-2}$  and amount of Pt,  $0.6 \text{ mg cm}^{-2}$

Pt at low potentials leads to the formation of linearly bonded CO species which are strongly adsorbed on the platinum surface and act as a catalyst poison. The surface reaction between this adsorbed CO species and adsorbed OH species, from water decomposition, causes the formation of carbon dioxide (final product of methanol oxidation) [8].

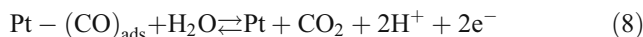
Generally accepted methanol oxidation process consists of the following steps that result in the formation of carboxyl intermediates and strongly adsorbed CO species [11, 24, 34, 35]:



Reactions 2 to 6 can be denoted by reaction 7:



The complete methanol oxidation (reaction 8) can occur and cause the sharp increase in current of methanol oxidation peak:



Cyclic voltammograms of 0.5 M methanol + 0.3 M  $\text{H}_2\text{SO}_4$  at Pt|CCE (optimum amount of Pt,  $2 \text{ mg cm}^{-2}$ ) (a), and Pt|PoPD|CCE (optimum amount of Pt,  $0.6 \text{ mg cm}^{-2}$ ) (b), were shown in Fig. 4. Onset potential of methanol oxidation is about 0.2 V and, by sweeping potential to the more positive values, the anodic peak of methanol oxidation appears (peak a). At high potentials, the oxidation of Pt and formation of platinum oxides causes a decrease in the amount of active sites available on the electrode surface that subsequently results in a decrease of peak current. In the backward scan, the reduction of platinum oxides to platinum and production of active sites take place, so re-oxidation of methanol and/or methanol residues occurs on clean platinum surface and backward peak (peak b) appears [36, 37]. The peak characteristics of cyclic voltammograms recorded for both two modified electrodes were given in Table 1. The peak potentials for both modified electrodes are nearly the same. Although the amount of Pt deposited at the CCE is more than three times ( $2 \text{ mg cm}^{-2}$ ) greater than that of Pt incorporated in the polymer film ( $0.6 \text{ mg cm}^{-2}$ ), but the peak currents of methanol oxidation at Pt|PoPD|CCE are greater than that of Pt|CCE. This demonstrates that a certain value of Pt nanoparticles can express different effective surface area depending on the nature of substrate. When the Pt particles dispersed into the PoPD film, the effective surface area of the catalyst increases with respect to the case of bare CCE and subsequently results in an increase in the electrocatalytic activity of them. Therefore, methanol oxidation study will be continuing at the Pt|PoPD|CCE.

### Effective parameters on the electrooxidation of methanol

*Effect of polymer amount* Figure 5a shows the anodic peak current of methanol oxidation as a function of polymer

**Table 1** The peak characteristics of cyclic voltammograms of methanol oxidation recorded at two kinds of modified electrodes

Electrode	Characteristics			
	$E_{\text{pa}}/\text{V}$	$E_{\text{pb}}/\text{V}$	$I_{\text{pa}}/\text{mA}$	$E_{\text{pb}}/\text{mA}$
Pt PoPD CCE	0.81	0.54	14.4	14
Pt CCE	0.88	0.49	13.3	9.4

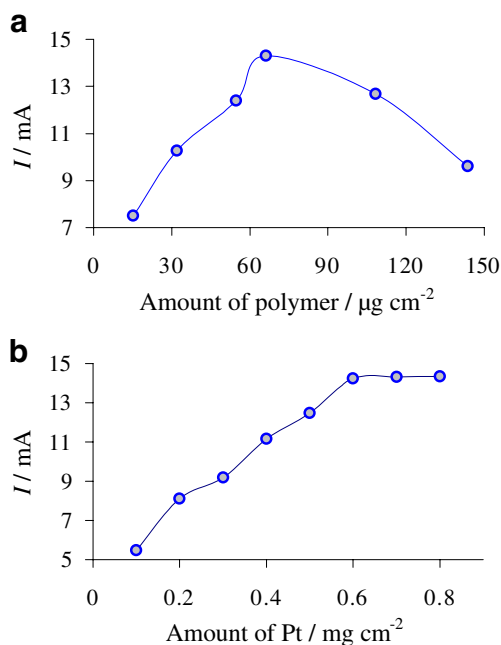


**Fig. 5** Plots of anodic peak current of Pt|PoPD|CCE in 0.3 M  $\text{H}_2\text{SO}_4$  solution containing 0.5 M methanol **a** as a function of the amount of polymer (Pt loading,  $0.6 \text{ mg cm}^{-2}$ ) and **b** as a function of platinum loading (amount of polymer,  $66 \mu\text{g cm}^{-2}$ ) derived from CVs with scan rate of  $50 \text{ mV s}^{-1}$

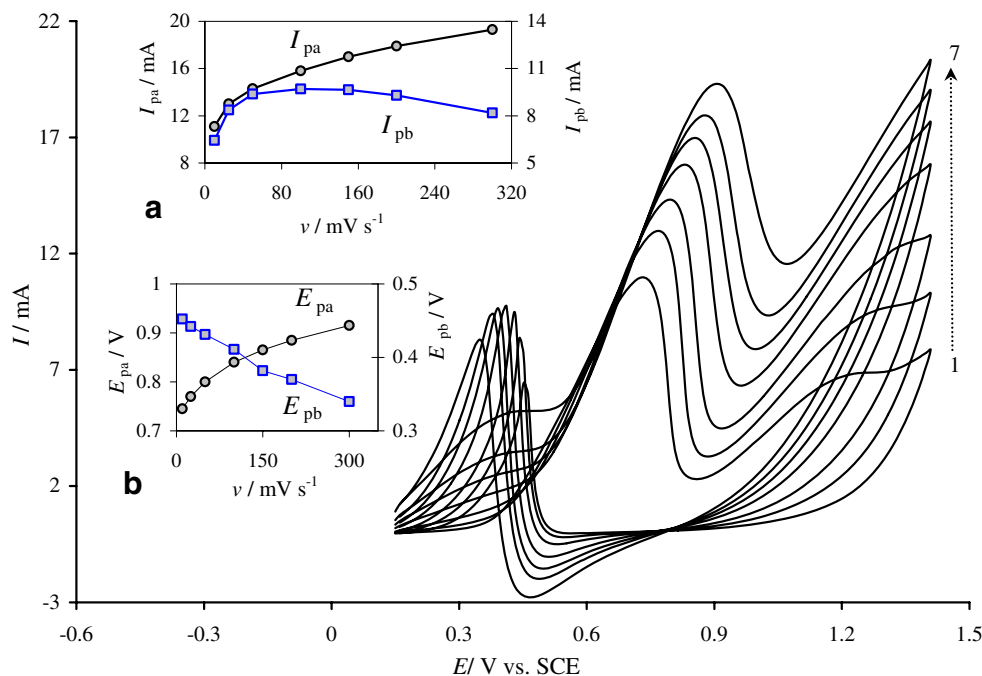
amount under the condition of constant Pt loading ( $0.6 \text{ mg cm}^{-2}$ ). The anodic current increases with increasing of the polymer amount up to about  $66 \mu\text{g cm}^{-2}$  and reached a maximum value for the amount of about  $66 \mu\text{g cm}^{-2}$  and then fell off with further increase in the amount of deposited polymer. The decrease in current may be attributed to the

reducing of the real surface area of Pt particles by the excessive presence of polymer on the electrode surface or reducing of polymer film conductivity in the higher amounts.

**Effect of platinum loading** The anodic current of methanol oxidation depends on the amount of Pt deposited on the PoPD film [38, 39]. The effect of different platinum loadings ranging from  $0.1$  to  $0.8 \text{ mg cm}^{-2}$  in the PoPD film on the oxidation of methanol was studied. Figure 5b indicates the variations of anodic peak currents vs. the amount of Pt loading (with the same amount of polymer film). As can be seen in Fig. 5b, the anodic current of methanol oxidation increases with increasing in the amount of Pt loading up to  $0.6 \text{ mg cm}^{-2}$  and levels off at higher amounts of Pt (most likely because of a constant active surface area of Pt particles). On the other hand, at the lower loadings of Pt, the active surface area of Pt particles increased in proportion to increasing Pt loading that causes an enhancement in the electrocatalytic activity of the modified electrode.

**Effect of scan rate** CVs of methanol oxidation on Pt|PoPD|CCE at different scan rates ( $\nu$ ) were shown in Fig. 6. In principle, peak currents are proportional to the  $\nu$  for an adsorption process and  $\nu^{0.5}$  for a diffusion process [40].  $I_{pa}$  increases with the scan rate in the range  $10\text{--}300 \text{ mV s}^{-1}$ , but there is not a clear dependence of  $I_{pa}$  on the scan rate (inset a to Fig. 6). In addition, the current of re-oxidation peak ( $I_{pb}$ ) increases with increasing scan rate up to  $100 \text{ mV s}^{-1}$  and then decreases for scan rates higher than  $100 \text{ mV s}^{-1}$

**Fig. 6** Cyclic voltammograms of Pt|PoPD|CCE in 0.3 M  $\text{H}_2\text{SO}_4$  containing 0.5 M methanol obtained at different scan rates (1–7), 10, 25, 50, 100, 150, 200, and  $300 \text{ mV s}^{-1}$ . Inset a variations of peak currents with scan rate. Inset b variations of peak potentials with scan rate. Amount of polymer film and amount of Pt were as in Fig. 2



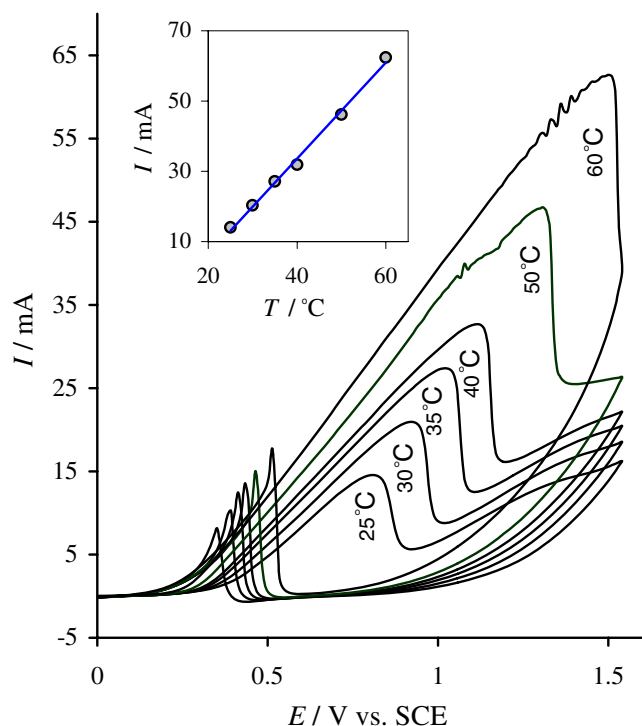


**Fig. 7** Cyclic voltammograms of Pt[PoPD]CCE in 0.3 M H<sub>2</sub>SO<sub>4</sub> containing 0.5 M methanol at different temperatures with scan rate of 50 mV s<sup>-1</sup>. Inset shows the variations of anodic peak currents with temperature. Amount of polymer and Pt were as in Fig. 2

(inset a to Fig. 6). These can be attributed to the acceleration of platinum surface oxidation in high scan rates; as a result in backward scans,  $I_{pb}$  reduces due to the low active sites available on the electrode surface [33]. The dependence of methanol oxidation peak potential ( $E_{pa}$ ) on the scan rate indicates an irreversible charge-transport process (inset b to Fig. 6) [40]. The potential of re-oxidation peak ( $E_{pb}$ ) shifts

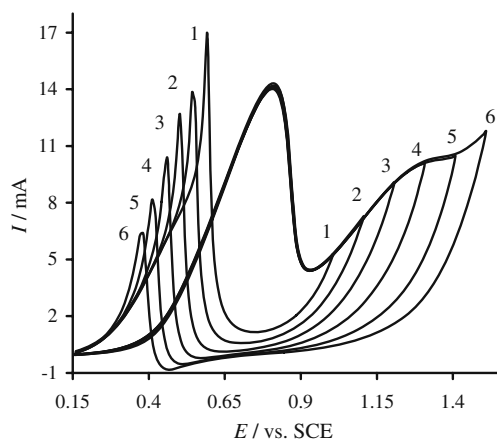


**Fig. 8** Cyclic voltammograms of Pt[PoPD]CCE in 0.3 M H<sub>2</sub>SO<sub>4</sub> containing 0.5 M methanol at different potential scan limits. 1 0.0–1.0 V, 2 0.0–1.1 V, 3 0.0–1.2 V, 4 0.0–1.3 V, 5 0.0–1.4 V, 6 0.0–1.5 V. Scan rate, 50 mV s<sup>-1</sup>; amount of polymer and Pt were as in Fig. 2

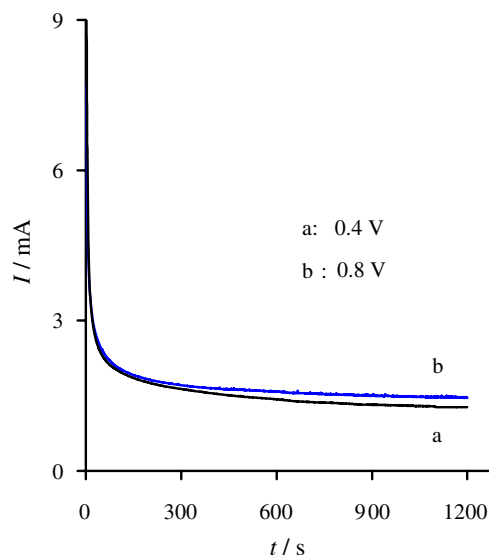


**Fig. 9** Long-time amperometric response of Pt[PoPD]CCE in stirring solution of 0.3 M H<sub>2</sub>SO<sub>4</sub> containing 0.5 M methanol, kept at different potentials; amount of polymer and Pt were as in Fig. 2

negatively with scan rate (inset b to Fig. 6) because most probably in high scan rates, the stability of platinum oxides increases, thus the reduction of them in backward scan needs more negative potentials.

Due to the fact that methanol oxidation commences by the water adsorption on the Pt and negative shift in potential of water adsorption with increasing scan rate [41], it can be said that the broad current peak in forward scan at potentials around 0.45 V is related to the adsorptive oxidation of water on the Pt surface.

*Effect of medium temperature* The effect of medium temperature on the electrooxidation of methanol was investigated. Figure 7 shows the cyclic voltammograms of

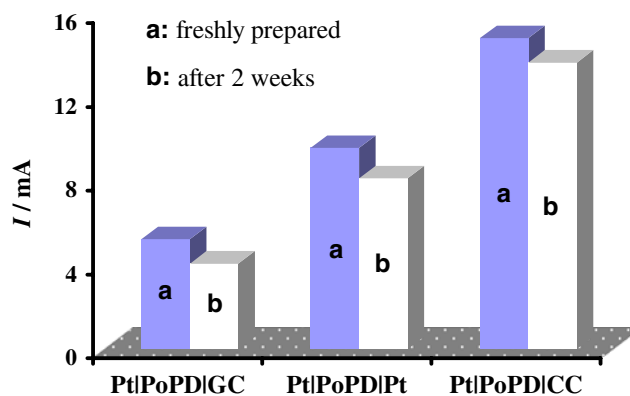
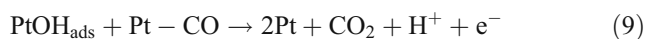


**Fig. 10** Histograms of anodic peak currents of methanol oxidation appeared at Pt[PoPD]GC, Pt[PoPD]Pt, and Pt[PoPD]CC electrodes in solution containing 0.3 M H<sub>2</sub>SO<sub>4</sub>+0.5 M CH<sub>3</sub>OH; scan rate, 50 mV s<sup>-1</sup>. Amount of polymer and Pt were as in Fig. 2

methanol oxidation on the surface of Pt|PoPD|CCE at different temperatures. Temperature dependence of methanol oxidation has been investigated previously [23, 32, 33, 41]. Inset to the Fig. 7 shows that an increase in temperature caused (1) an evident increase in the anodic peak current for methanol oxidation up to 60 °C, indicating acceleration of methanol oxidation kinetics with temperature and (2) a negative shift in the onset potential and a positive shift in the re-oxidation peak potential are observed. These may be attributed to the facilitating effect of higher temperature on the adsorption of water molecule on Pt particles and desorption of oxide species from Pt surface.

*Effect of forward potential scan limit* Figure 8 shows cyclic voltammograms of methanol oxidation on Pt|PoPD|CCE for different final potential scan limit. As can be seen in Fig. 8, extending the anodic potential limit to the positive direction in forward scan caused a significant decrease in the current of re-oxidation peak in backward scan. As mentioned before, the re-oxidation peak of methanol is related to the oxidation of methanol and/or methanol residues (Pt–C≡O) in backward scan. The reaction of re-oxidation peak is assumed as follows [37]:



Extending the potential window to the positive direction in forward scan accelerates the formation of oxide species (e.g., platinum oxides) and causes a decrease in the re-oxidation peak current [33, 42]. Also, by increasing the forward potential scan limit, re-oxidation peak potential shifts negatively because of stabilizing of oxidative platinum surfaces in high potentials and difficult reduction of them in backward scan.

### Chronoamperometric studies

In order to evaluate the electrocatalytic activity of the catalyst and the poisoning of the active surface under continuous operation conditions, long-term chronoamperometry experiments were performed. Figure 9 shows the chronoamperograms of Pt|PoPD|CCE in 0.3 M H<sub>2</sub>SO<sub>4</sub> containing 0.5 M CH<sub>3</sub>OH after stepping the electrode potential from an initial value of 0.05 to 0.4 V (curve a) and 0.8 V (curve b) vs. SCE. As can be seen in the Fig. 9, in both curves, the currents dropped rapidly at first, and then the currents became relatively stable, due to the fast poisoning of Pt surface by adsorbed intermediates [43]. The current of plateau at potential of 0.8 V (curve b) is higher than that of 0.4 V (curve a) because its potential is

close to the potential of the anodic peak in the CV (see Fig. 4b). In addition, the stability of plateau current at 0.8 V is the most; this can be probably attributed to the low poisoning effect at 0.8 V in comparison with 0.4 V.

Finally, we investigated the electrooxidation of methanol at the surface of PoPD-modified CC, Pt, and GC electrodes containing the same amount of Pt catalyst. Figure 10 shows the anodic currents of methanol electrooxidation under the same conditions at the surface of these electrodes, (a) immediately after preparation of electrodes and (b) after storing of them for 2 weeks in the laboratory atmosphere. The comparison of results related to the same platinum values loaded into the PoPD modified electrodes (i.e., Pt|PoPD|CC, Pt|PoPD|GC, and Pt|PoPD|Pt electrodes) indicates clearly that the Pt|PoPD|CC electrode yields higher current than other platinized PoPD-modified electrodes. The high current and relatively high stability of Pt|PoPD|CC electrode may be originated from the scaly nature of carbon ceramic in comparison with other substrates (GC and Pt). The CCE surface induced the formation of high porous polymer film with high adhesion to the carbon ceramic substrate, so the configuration of the deposited platinum particles on the polymer changes, which appears as a decrease in the average particle size and an increase in the specific surface area of the electrode.

### Conclusions

Carbon ceramic acts as a suitable substrate for electrosynthesis of PoPD. Platinum nanoparticles incorporated into the PoPD film improved electrochemical characteristics for the oxidation of methanol in acidic medium. The Pt|PoPD|CCE showed a moderate increase in the Pt-normalized current compared to the platinum-coated carbon ceramic electrode (Pt|CCE). In addition, the catalytic activity of Pt-coated PoPD film on the CCE surface was better than GC or Pt electrodes. The prepared electrodes exhibited satisfactory stability and reproducibility if they were stored in ambient conditions.

**Acknowledgments** The authors wish to express their gratitude to the research office of Azarbaijan University of Tarbiat Moallem for supporting this work.

### References

1. Wasmus S, Kuver A (1999) J Electroanal Chem 461:14. doi:10.1016/S0022-0728(98)00197-1
2. Ren XM, Zelenay P, Thomas S, Davey J, Gottesfeld S (2000) J Power Sources 86:11. doi:10.1016/S0378-7753(99)00407-3
3. Steele BCH, Heinzel A (2001) Nature 414:345. doi:10.1038/35104620

4. Ribeiro J, Dos Anjos DM, Kokoh KB, Coutanceau C, Léger JM, Olivi P, De Andrade AR, Tremiliosi-Filho G (2007) *Electrochim Acta* 52:6997. doi:10.1016/j.electacta.2007.05.017
5. Wang ZB, Yin GP, Lin YG (2007) *J Power Sources* 170:242. doi:10.1016/j.jpowsour.2007.03.078
6. Li H, Sun G, Cao L, Jiang L, Xin Q (2007) *Electrochim Acta* 52:6622. doi:10.1016/j.electacta.2007.04.056
7. Wang H, Jusys Z, Behm RJ (2006) *J Power Sources* 154:351. doi:10.1016/j.jpowsour.2005.10.034
8. Léger JM, Rousseau S, Coutanceau C, Hahn F, Lamy C (2005) *Electrochim Acta* 50:5118. doi:10.1016/j.electacta.2005.01.051
9. Santhosh P, Gopalan A, Vasudevan T, Lee KP (2006) *Appl Surf Sci* 252:7964. doi:10.1016/j.apsusc.2005.10.002
10. Golabi SM, Nozad A (2002) *J Electroanal Chem* 521:161. doi:10.1016/S0022-0728(02)00656-3
11. Niu L, Li Q, Wei F, Wu S, Liu P, Cao X (2005) *J Electroanal Chem* 578:331. doi:10.1016/j.jelechem.2005.01.014
12. Lenoé A, Marino W, Scharifker BR (1992) *J Electrochem Soc* 139:438. doi:10.1149/1.2069236
13. Zhong Q, Xiong L, Zhong Z, Li W (1996) *Acta Physchim Sin* 12:351
14. Mikhaylova AA, Molodkina EB, Khazova OA, Bagotzky VS (2001) *J Electroanal Chem* 509:119. doi:10.1016/S0022-0728(01)00479-X
15. Castro Luna AM (2000) *J Appl Electrochem* 30:1137. doi:10.1023/A:1004050922065
16. Rajendra Prasad K, Munichandraiah N (2002) *J Power Sources* 103:300. doi:10.1016/S0378-7753(01)00841-2
17. Niu L, Li Q, Wei F, Chen X, Wang H (2003) *J Electroanal Chem* 544:121. doi:10.1016/S0022-0728(03)00085-8
18. Bouzek K, Mangold KM, Jüttner K (2001) *J Appl Electrochem* 31:501. doi:10.1023/A:1017527114207
19. Hammache H, Makhloufi L, Saidani B (2001) *Synth Met* 123:515. doi:10.1016/S0379-6779(01)00345-9
20. Biallozor S, Kupniewska A, Jasulaitene V (2003) *Fuel Cells (Weinh)* 3:8. doi:10.1002/fuce.200320242
21. Yassar A, Roncali J, Garnier F (1988) *J Electroanal Chem* 225:53. doi:10.1016/0022-0728(88)80004-4
22. Swathirajan S, Mikhail YM (1992) *J Electrochem Soc* 139:2105. doi:10.1149/1.2221186
23. Golikand AN, Golabi SM, Ghannadi Maragheh M, Irannejad L (2005) *J Power Sources* 145:116. doi:10.1016/j.jpowsour.2005.02.061
24. Pournaghi-Azar MH, Habibi B (2007) *J Electroanal Chem* 601:53. doi:10.1016/j.jelechem.2006.10.027
25. Lei CX, Yang Y, Wang H, Shen GL, Yu RQ (2004) *Anal Chim Acta* 513:379. doi:10.1016/j.aca.2004.01.029
26. Oskam G, Searson PC (1998) *J Phys Chem B* 102:2464. doi:10.1021/jp972313v
27. Yang XH, Hua L, Gong HQ, Tan SN (2003) *Anal Chim Acta* 478:67. doi:10.1016/S0003-2670(02)01507-6
28. Shankaran DR, Uehera N, Kato T (2002) *Anal Bioanal Chem* 374:412. doi:10.1007/s00216-002-1507-4
29. Razmi H, Habibi E, Heidari H (2008) *Electrochim Acta* 53:8178. doi:10.1016/j.electacta.2008.06.033
30. Nichols RJ, Bewick A (1988) *J Electroanal Chem* 243:445. doi:10.1016/0022-0728(88)80047-0
31. Ren B, Xu X, Li XQ, Cai WB, Tian ZQ (1999) *Surf Sci* 427:157. doi:10.1016/S0039-6028(99)00257-5
32. Pournaghi-Azar MH, Habibi B (2005) *J Electroanal Chem* 580:23. doi:10.1016/j.jelechem.2005.02.021
33. Noazd Golikand A, Ghannadi Maragheh M, Sedaghat Sherehjini S, Taghi-Ganji KM, Yari M (2006) *Electroanalysis* 18:911. doi:10.1002/elan.200503476
34. Vigier F, Gloaguen F, Léger JM, Lamy C (2001) *Electrochim Acta* 46:4331. doi:10.1016/S0013-4686(01)00680-6
35. Ross P, Markovic N (2000) *CATTECH* 4:110. doi:10.1023/A:1011963731898
36. Li WS, Tian LP, Huang QM, Li H, Chen HY, Lian XP (2002) *J Power Sources* 104:281. doi:10.1016/S0378-7753(01)00961-2
37. Manohara R, Goodenough JB (1992) *J Mater Chem* 2:875. doi:10.1039/jm9920200875
38. Kulesza PJ, Matczak M, Wieckowski A (1999) *Electrochim Acta* 44:2131. doi:10.1016/S0013-4686(98)00321-1
39. Xue KH, Cai CX, Yang H, Sun SG (1998) *J Power Sources* 75:207. doi:10.1016/S0378-7753(98)00098-6
40. Bard AJ, Faulkner LR (2001) *Electrochemical methods*. Wiley, New York, p 226
41. Lee CG, Umeda M, Uchida I (2006) *J Power Sources* 160:78. doi:10.1016/j.jpowsour.2006.01.068
42. Pournaghi-Azar MH, Habibi B (2007) *J Electroanal Chem* 605:136. doi:10.1016/j.jelechem.2007.03.025
43. Kabbabi A, Faure R, Durand R, Beden B, Hahn F, Léger JM, Lamy C (1998) *J Electroanal Chem* 444:41. doi:10.1016/S0022-0728(97)00558-5